'The Physics and Chemistry of the Heaviest Elements',
Workshop, 14-18 September 2026, Trento

A recent experimental fission study of a superheavy nucleus

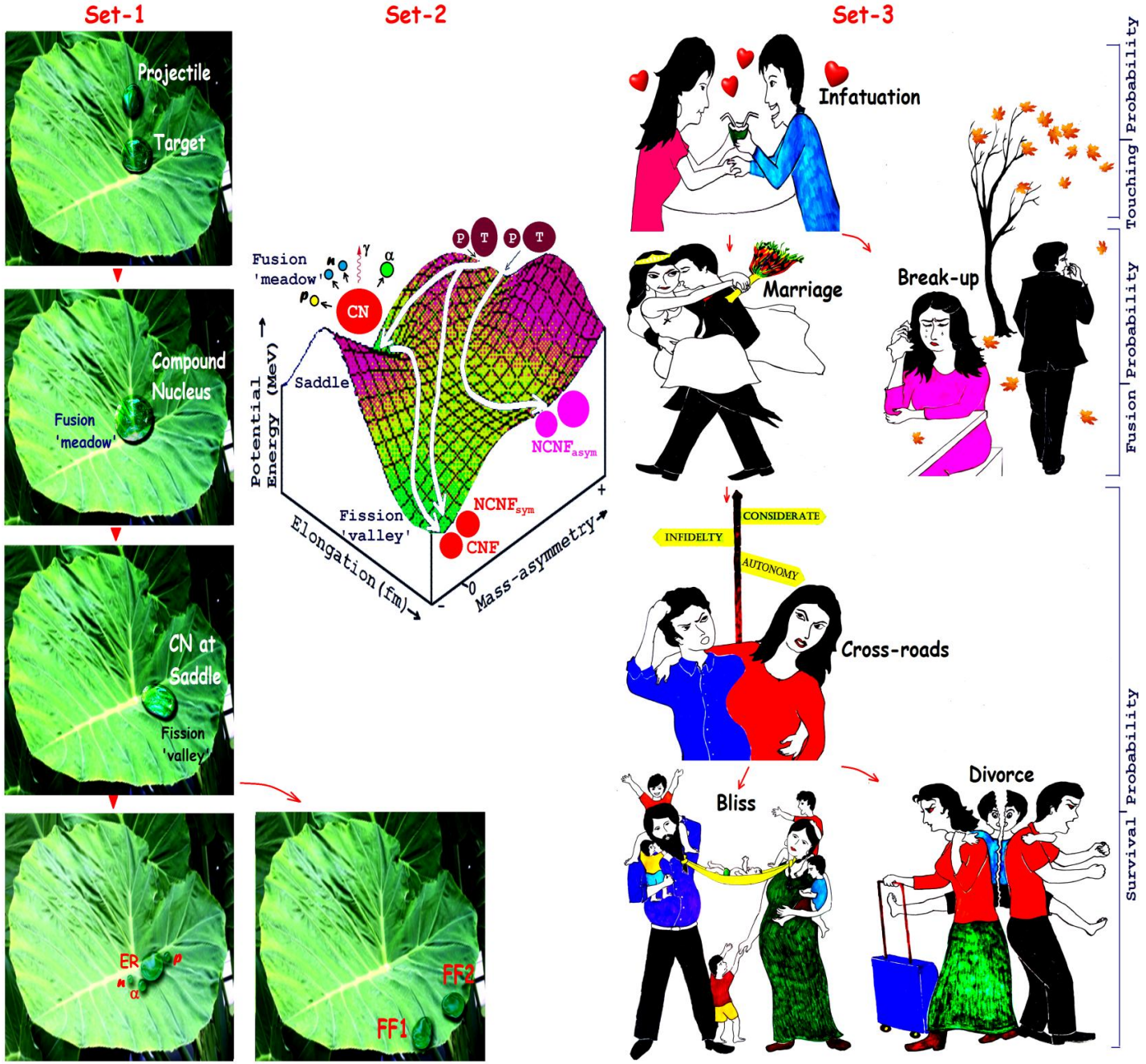
Tathagata Banerjee (INFN, Napoli, Italy)

Istituto Nazionale di Fisica Nucleare

Università degli Studi di Napoli Federico II

he.tatha@gmail.com

Introduction



$$\sigma_{\mathrm{ER}}(E_{\mathrm{c.m.}}) = \sum_{\ell=0}^{\infty} \sigma_{\mathrm{cap}}(E_{\mathrm{c.m.}}, \ell) P_{\mathrm{CN}}(E_{\mathrm{c.m.}}, \ell) P_{\mathrm{sur}}(E^*, \ell).$$

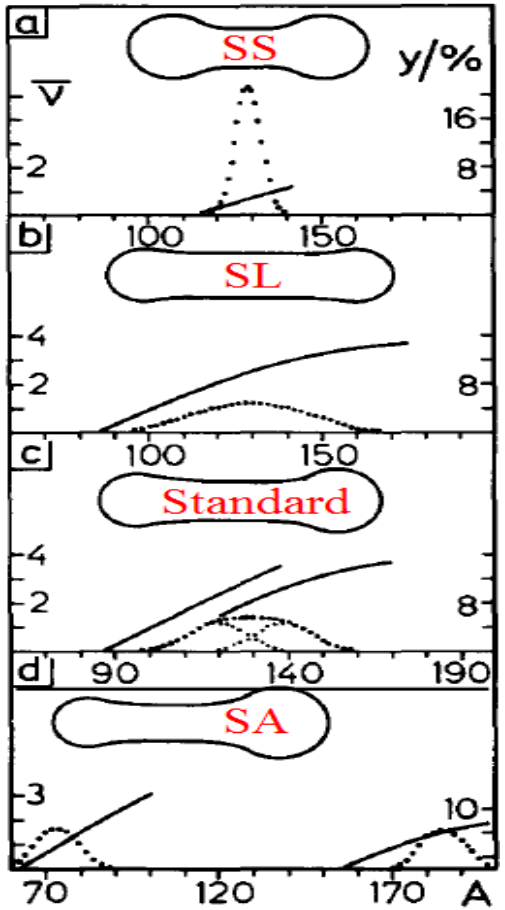
he.tatha@gmail.com

Introduction

- The nucleus may choose among various paths to disintegration leaving the compound state.

- Fission modes by Brosa et al.:

Symmetric	**Superlong (SL)**	
	Supershort (SS)	**Z ~50, N~82**
Asymmetric	**Standard 1 (S1)**	**Z ~50, ~53, N~82**
	Standard 2 (S2)	**Z~55, 82; N~88, 126**
	Standard 3 (S3)	**N~50**
	Super-asymmetric (SA)	**Z~28**



short prescission shape -> high TKE

long prescission shape -> low TKE



Ulrich Brosa, Siegfried Grossmann, and Andreas Muller, Phys. Rep. 197, 167 (1990).

he.tatha@gmail.com

Motivation

- **Cold fusion reactions** with Pb or Bi targets ⇨ a route to the **superheavy elements (SHE)**
  - the projectile and target are often (near-) magic nuclei [e.g., ^{48}Ca (Z=20, N=28), ^{208}Pb (Z=82, N=126), ^{209}Bi]
  - enhanced shell binding reduces the excitation energy

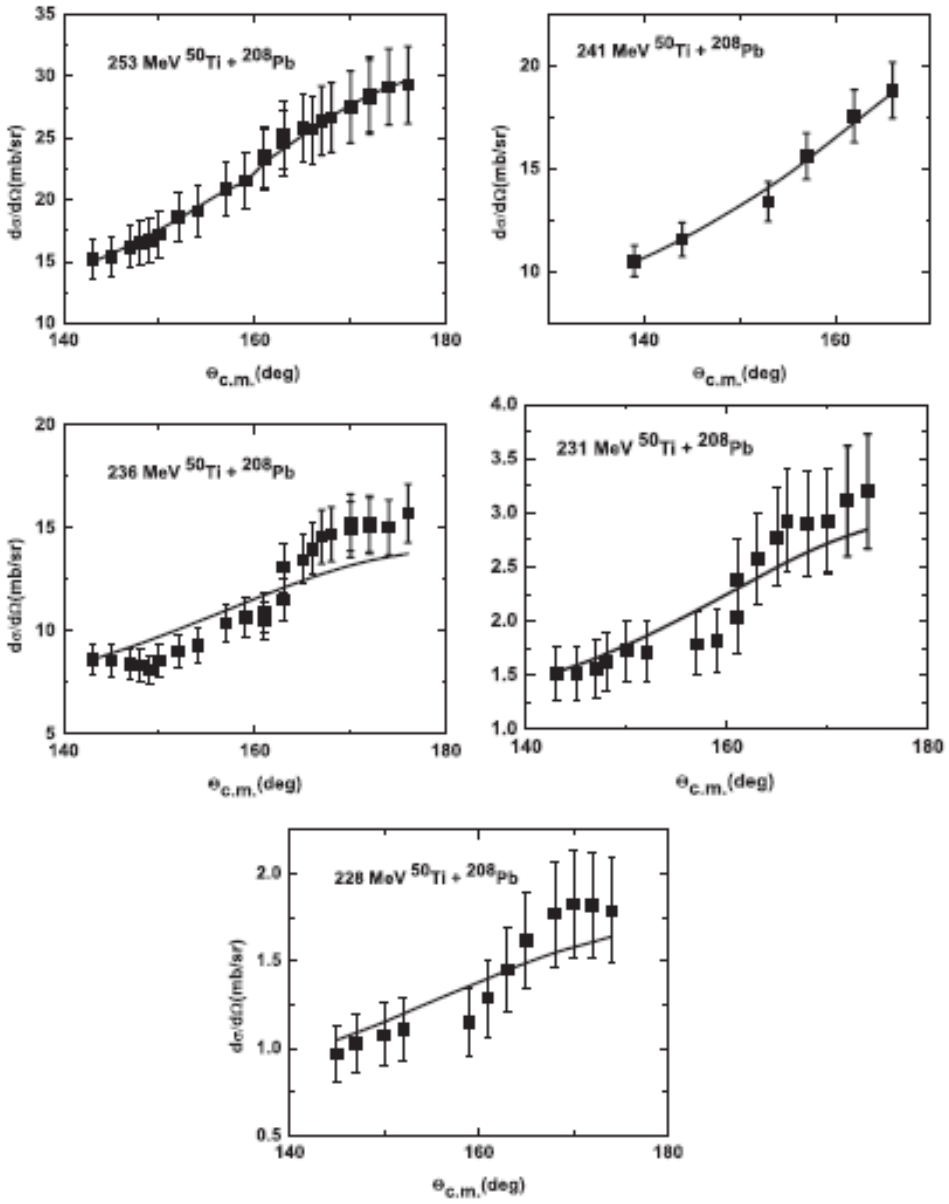
- **Such shell effects can steer mass dist. toward preferred mass splits**
  - associated with shell-stabilized configurations (e.g., spherical, cigarlike, and pearlike shapes).

- **Fusion probability is governed not only by shell effects (magicity)**
  - but also by factors such as isospin asymmetry, and nuclear deformation.

- **The precise quantification of fusion suppression** in heavy-projectile induced reactions is **obscured**
  - by dominant non-compound processes, limited data, and uncertain models.

- **The extraction of P_{CN}** from exp. data:
  - performed **for only a few cold fusion reactions** with ^{208}Pb target
  - **P_{CN} cannot be measured directly. It is inferred.**

Motivation



Fission fragment angular distribution

$$W(\theta) = \sum_{J=0}^{J_{CN}} \frac{(2J+1)^2 \exp\left[-(J+1/2)^2 \sin^2\theta / 4K_0^2(FF)\right] J_0\left[i(J+1/2)^2 \sin^2\theta / 4K_0^2(FF)\right]}{erf\left[(J+1/2)/\left(2K_0^2(FF)\right)^{1/2}\right]}$$
$$+ \sum_{J=J_{CN}}^{J_{max}} \frac{(2J+1)^2 \exp\left[-(J+1/2)^2 \sin^2\theta / 4K_0^2(QF)\right] J_0\left[i(J+1/2)^2 \sin^2\theta / 4K_0^2(QF)\right]}{erf\left[(J+1/2)/\left(2K_0^2(QF)\right)^{1/2}\right]}$$

$$\frac{\Im_0}{\Im_{eff}} = 1.5 \quad \text{for} \quad J \succ J_{cn}$$

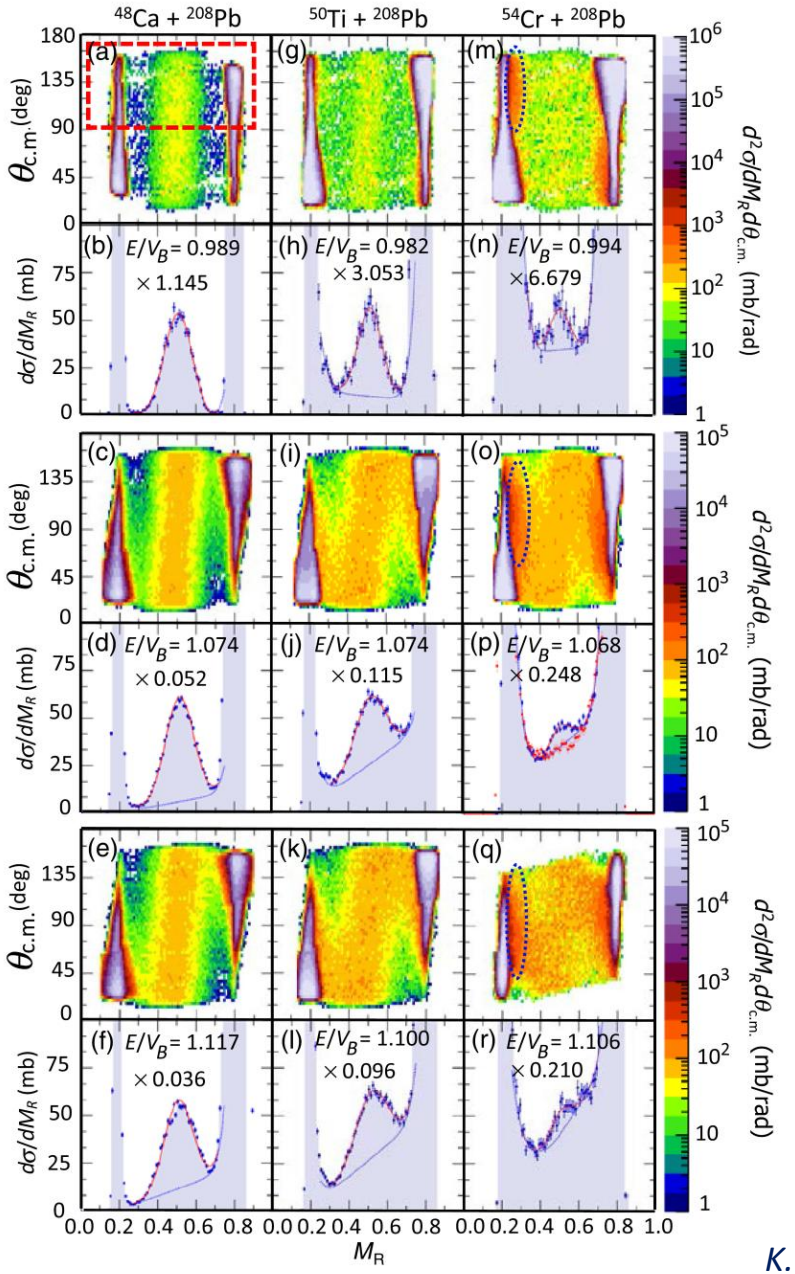
$$\frac{J_{CN}^2}{J_{max}^2} = \frac{\sigma_{CN}}{\sigma_{capture}} = P_{CN}$$

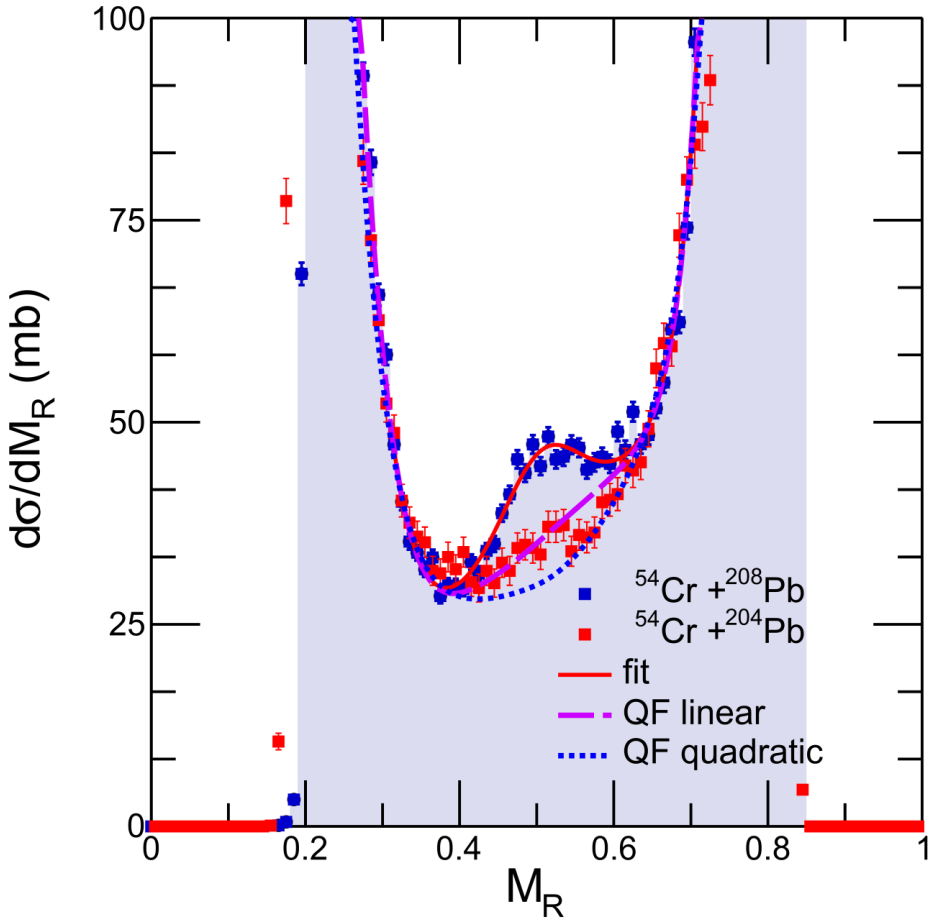
Error may arise from:

- the choice of the effective moment of inertia for quasifission,
- the estimation of maximum angular momentum associated with the total fission cross section
  - specially if there is no precisely measured data available for the same reaction.

R. S. Naik et al., Phys. Rev. C 76, 054604 (2007).

Motivation





Fission fragment mass angle distribution

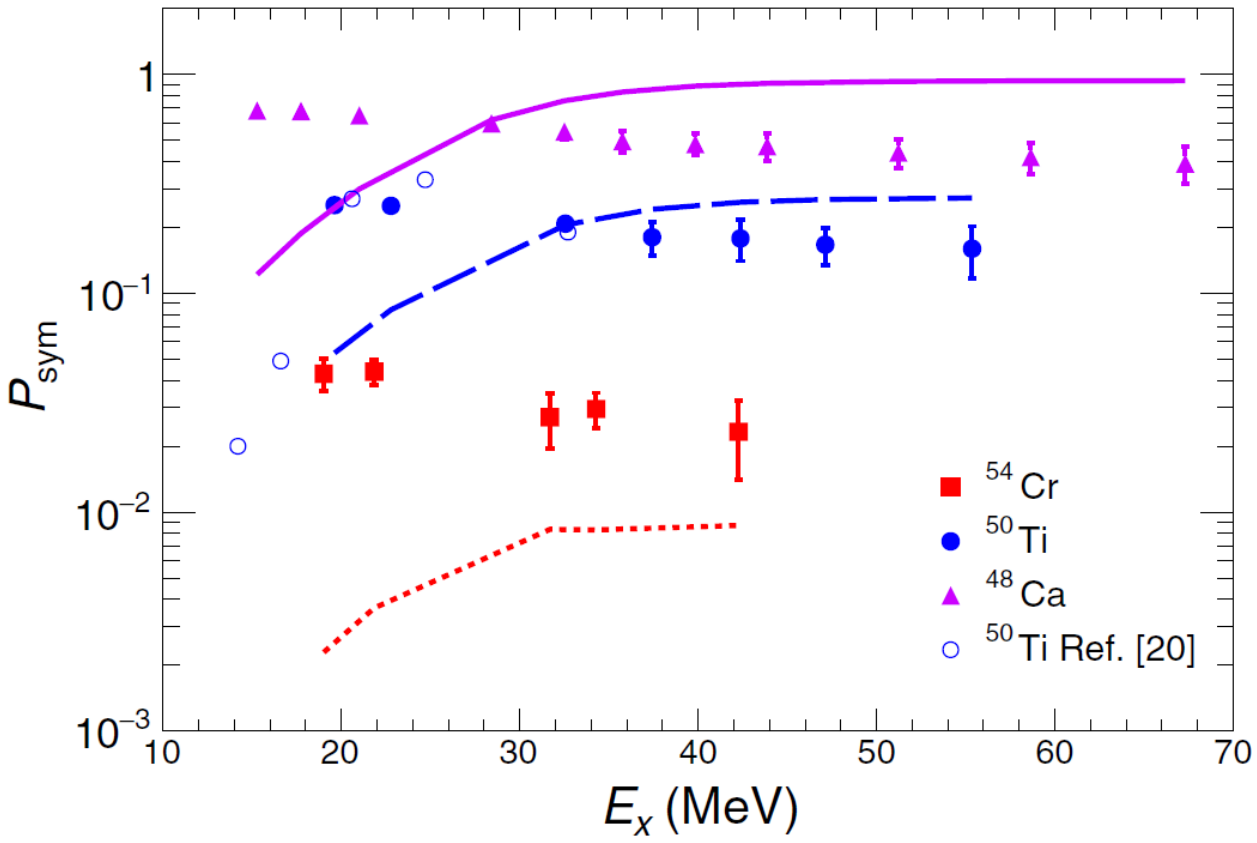
- If no symmetric peak is visible?
- Systematic errors can arise from the assumed background shape!

$$P_{CN} = \sigma_{FF}/\sigma_{capture} < (\sigma_{FF} + \sigma_{SQF})/\sigma_{capture}$$

$$P_{sym} = \frac{\sigma_{sym}}{\sigma_c} = \frac{\sigma_{sym}}{\sigma_{fis}/S}$$

K. Banerjee et al., Phys. Rev. Lett. 122, 232503 (2019)

Motivation



- A consistent understanding of the reaction mechanism requires considering **P_{CN} together with the underlying shell-driven dynamics**.

- The evolution of competing nuclear processes **measuring the mass-total kinetic energy (MTKE) for ^{54}Cr+^{209}Bi** of fission fragments at three beam energies

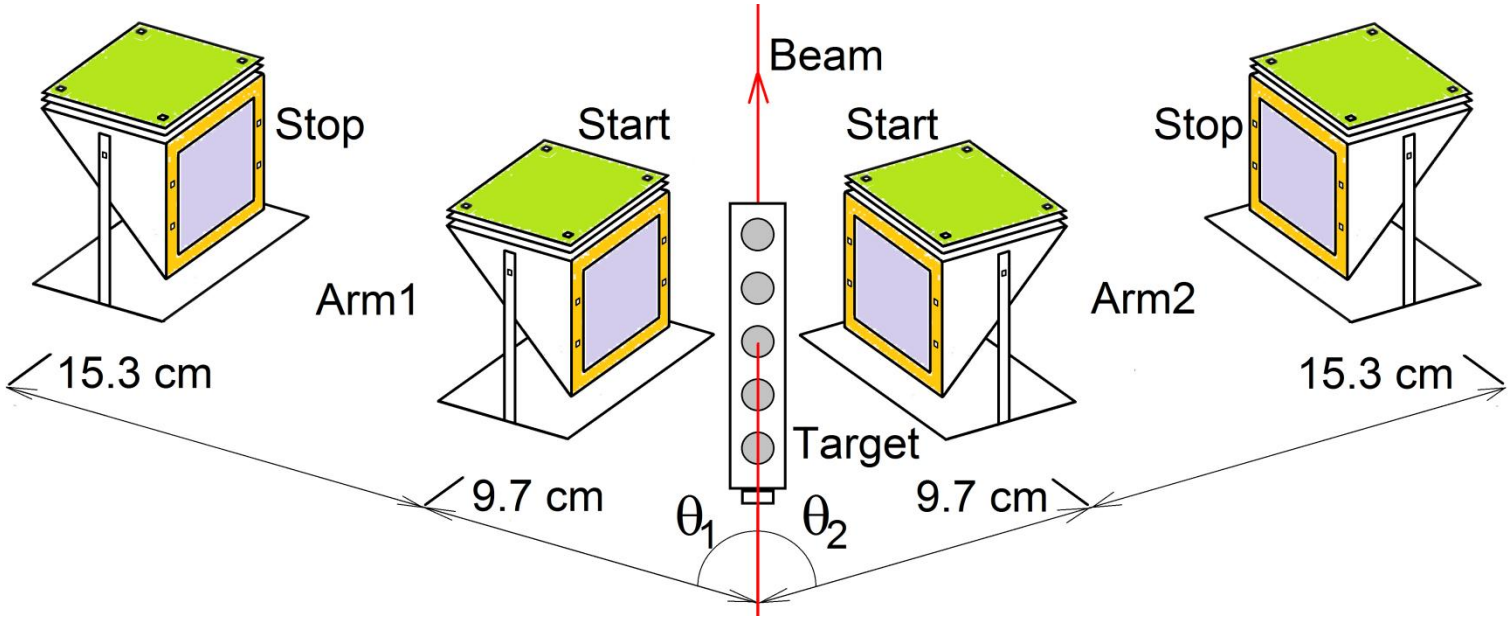
- **Analyze the P_{CN} values for ^{54}Cr+^{209}Bi**, with the aim of alleviating the mentioned ambiguities.

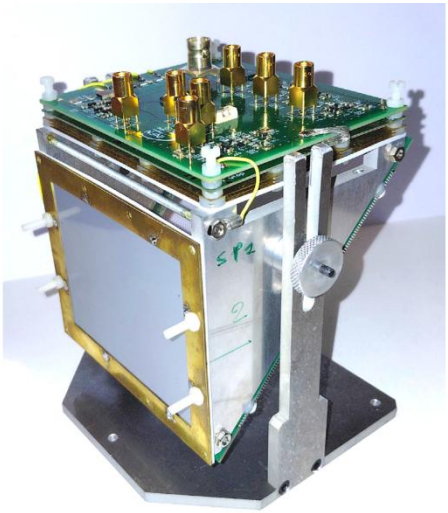
- **Identify possible active shell effects** influencing the fission dynamics

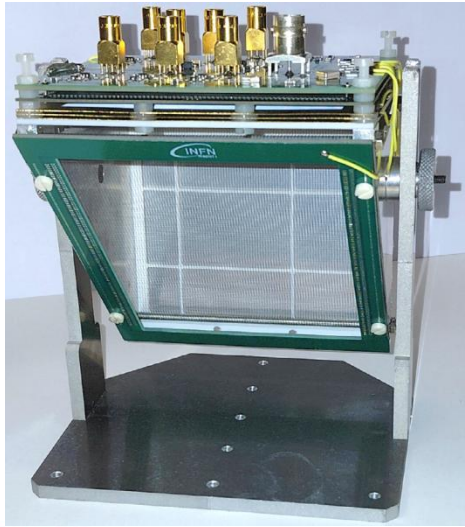
K. Banerjee et al., Phys. Rev. Lett. 122, 232503 (2019)

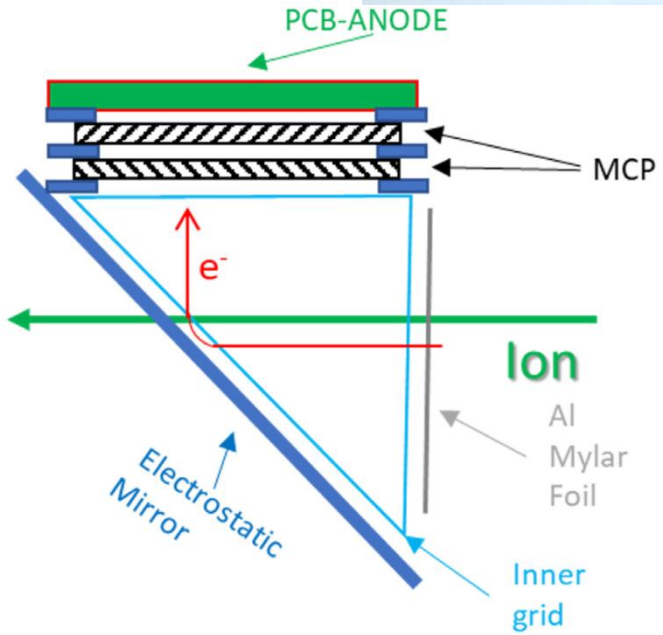
Experimental details

Measurements were carried out at the Accelerator Laboratory at the University of Jyväskylä



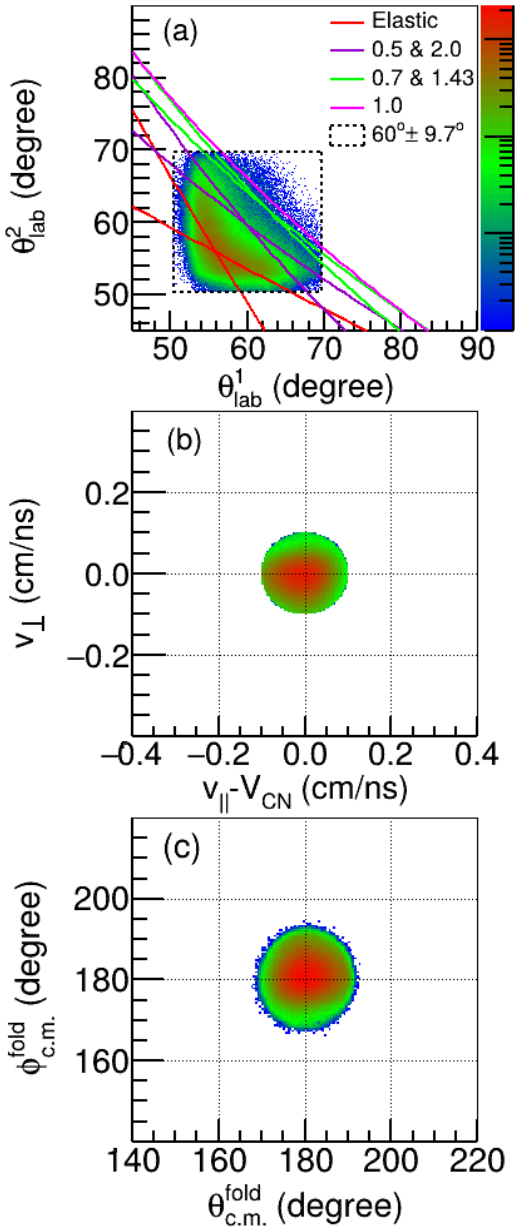






E. Vardaci, A. Vanzanella, T. Banerjee, A. Di Nitto et al., Nucl. Instrum. Methods Phys. Res. A 1091, 171746 (2026).
T. Banerjee, E. Vardaci, A. Di Nitto et al., Phys. Rev. Lett. 137, 062501 (2026)

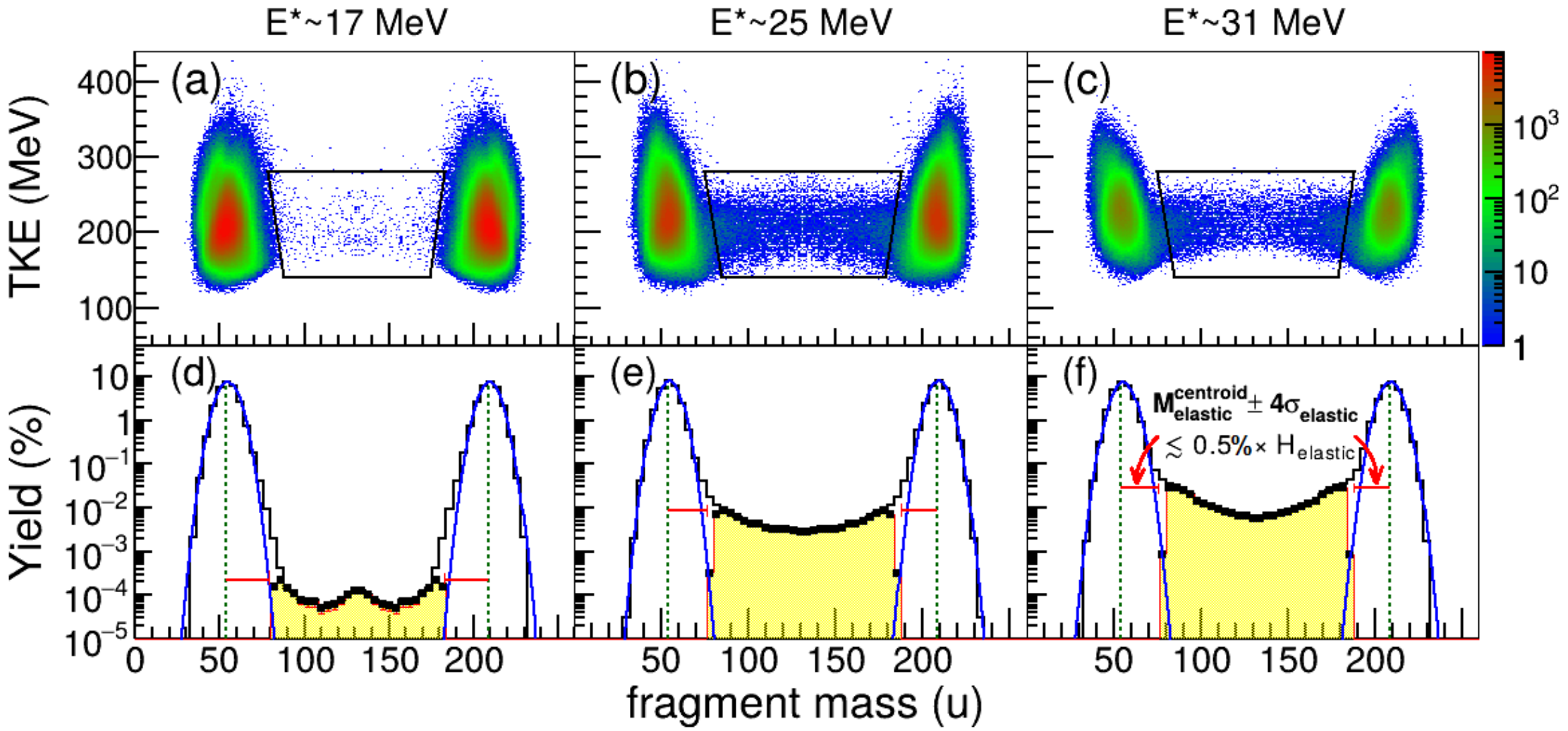
Angular correlation plot $(\theta\text{-}\phi)_{lab}$, velocity $(V_{||}\text{-}V_{\perp})$ distribution, folding angle $(\theta^{fold}\text{-}\phi^{fold})_{c.m.}$ distribution of $^{54}Cr+^{209}Bi \rightarrow {}^{263}Bh$ at E_{lab}= 278 MeV



- Panel (a):
  - **Measured angular correlation plot along with the calculated correlation** curves in dependence on the mass ratio (R) of the two fragments
    - e.g. R = 1 refers to symmetric fragmentation of a composite system. The red lines are for elastic scattering.
  - The black dotted box indicated the **detector coverage** into which the present data were accumulated.
- Panel (b):
  - **Gated velocity $(V_{||}\text{-}V_{\perp})$ distribution**. A circular gate of 0.1 cm/ns was put to select only full momentum transfer (FMT) events.
- Panel (c):
  - **Velocity gated folding angle** $(\theta^{fold}\text{-}\phi^{fold})_{c.m.}$ distribution.

T. Banerjee, E. Vardaci, A. Di Nitto et al., Phys. Rev. Lett. 137, 062501 (2026)

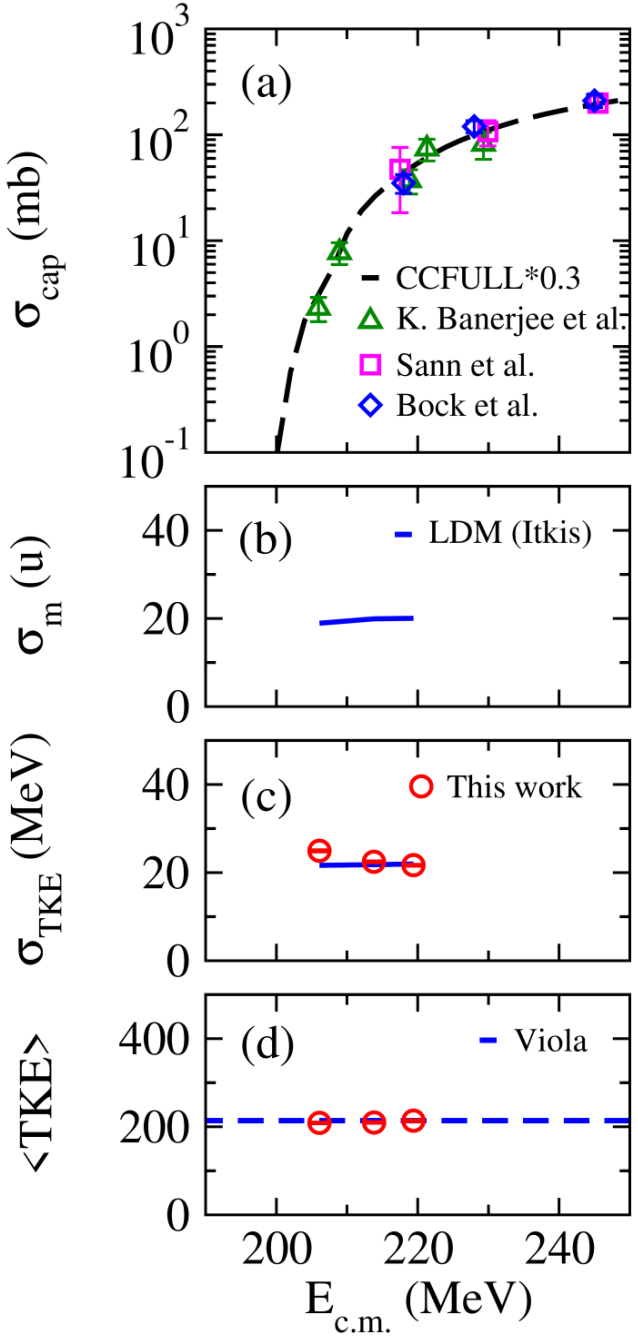
Velocity Gated Mass-TKE distributions of $^{54}Cr+^{209}Bi \rightarrow {}^{263}Bh$ at E_{beam}= 261, 271, and 278 MeV



$$M^{\text{lower}}_{\text{elastic}} + 4\sigma_{\text{elastic}} < M < M^{\text{upper}}_{\text{elastic}} - 4\sigma_{\text{elastic}}$$

T. Banerjee, E. Vardaci, A. Di Nitto et al., Phys. Rev. Lett. 137, 062501 (2026)

Width calculation for mass and TKE

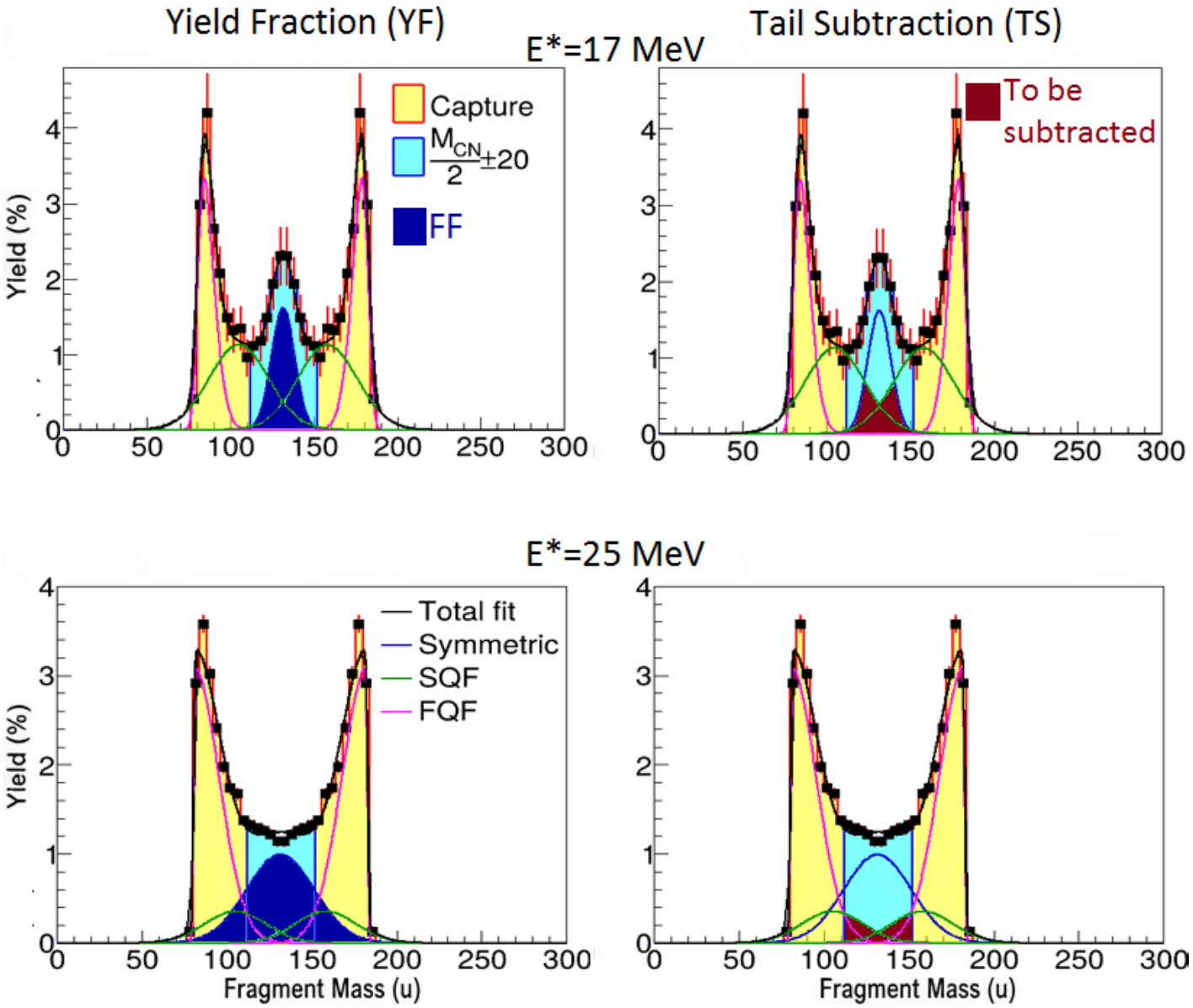


- The $\langle l^2 \rangle$ is calculated after matching the measured capture (or fission) cross sections with the coupled cannel code CCFULL.

- This $\langle l^2 \rangle$ is then used to calculate the LDM predictions of the widths of the mass and TKE for the symmetric events using Itkis systematics.

M. G. Itkis and A. Y. Rusanov, Phys. Part. Nucl. 29, 160 (1998).
V. E. Viola, Jr., Nucl. Data Sheets, Sect. A 1, 391 (1965).
T. Banerjee, E. Vardaci, A. Di Nitto et al., Phys. Rev. Lett. 137, 062501 (2026)

Methods for extracting FF



- The Gaussian tails and their overlap reflect underlying physical processes rather than fitting artifacts,

Although their quantitative extent depends on the fitting constraints.

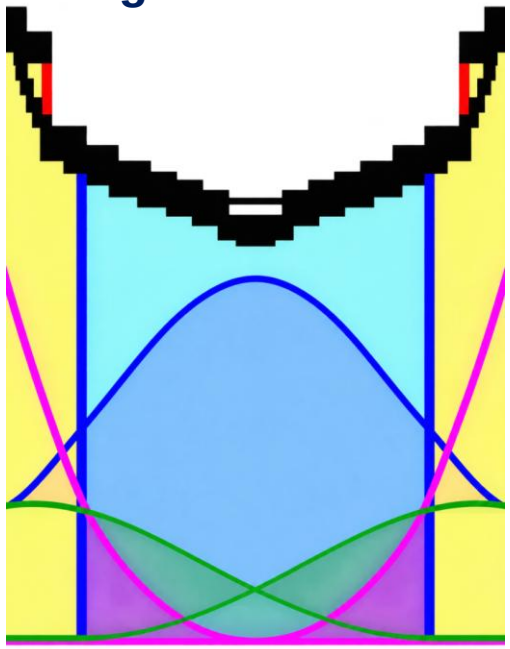
$$f_{blue}^{upper} = \frac{\int B(x)\,dx}{\int \sum_j F_j(x)\,dx},$$

- Interpreting YFs as true probabilities is unjustified when the FF component is substantially or fully buried, leaving them only as upper limits.

T. Banerjee, E. Vardaci, A. Di Nitto et al., Phys. Rev. Lett. 137, 062501 (2026)

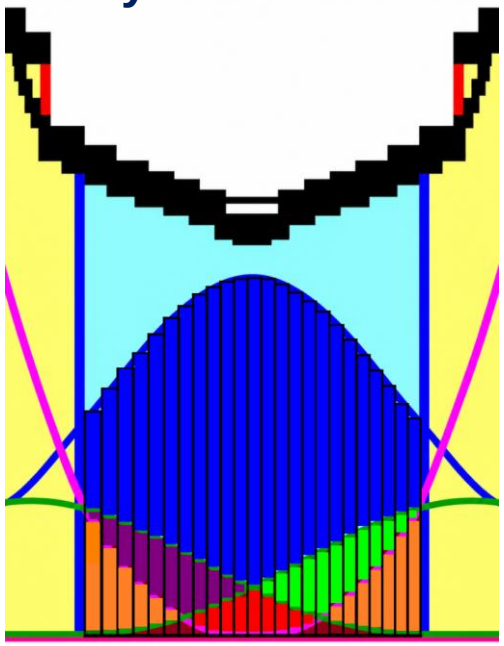
Different methods of tail subtraction for extracting FF

Integral Subtraction



$$A_{blue}^{tail,\,sym} = \int_{x_{min}^{sym}}^{x_{max}^{sym}} B(x)\,dx - \sum_i \int_{x_{min}^{sym}}^{x_{max}^{sym}} N_i(x)\,dx\,,$$

Bin-by-bin Subtraction

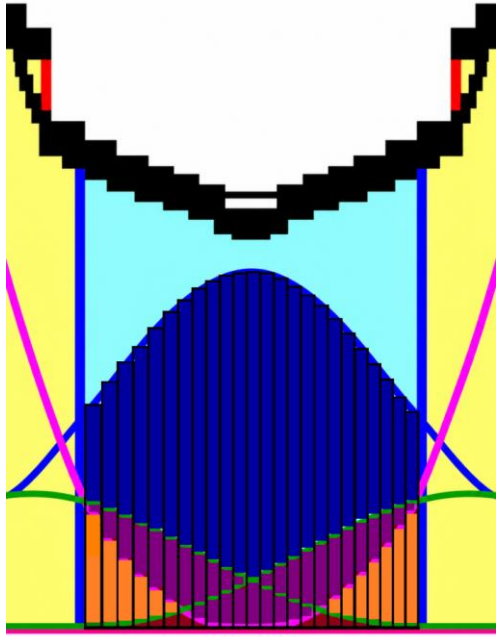


$$A_{blue}^{sym} \approx \sum_{k=1}^{N_{sym}} \max\left[B(x_k) - \sum_i N_i(x_k),\, 0\right] \Delta x_{sym},$$

$$x_k = x_{min}^{sym} + \left(k - \frac{1}{2}\right) \Delta x_{sym},$$

$$\Delta x_{sym} = \frac{x_{max}^{sym} - x_{min}^{sym}}{N_{sym}}.$$

Maximal Subtraction



$$A_{blue}^{max} = \sum_k \max\left[B(x_k) - \max_i N_i(x_k),\, 0\right] \Delta x,$$

$$> \sum_k \max\left[B(x_k) - \sum_i N_i(x_k),\, 0\right] \Delta x = A_{blue}^{unamb}$$

T. Banerjee, E. Vardaci, A. Di Nitto et al., Phys. Rev. Lett. 137, 062501 (2026)

$\max(SQF,FQF) \leq (SQF+FQF)$ for each bin

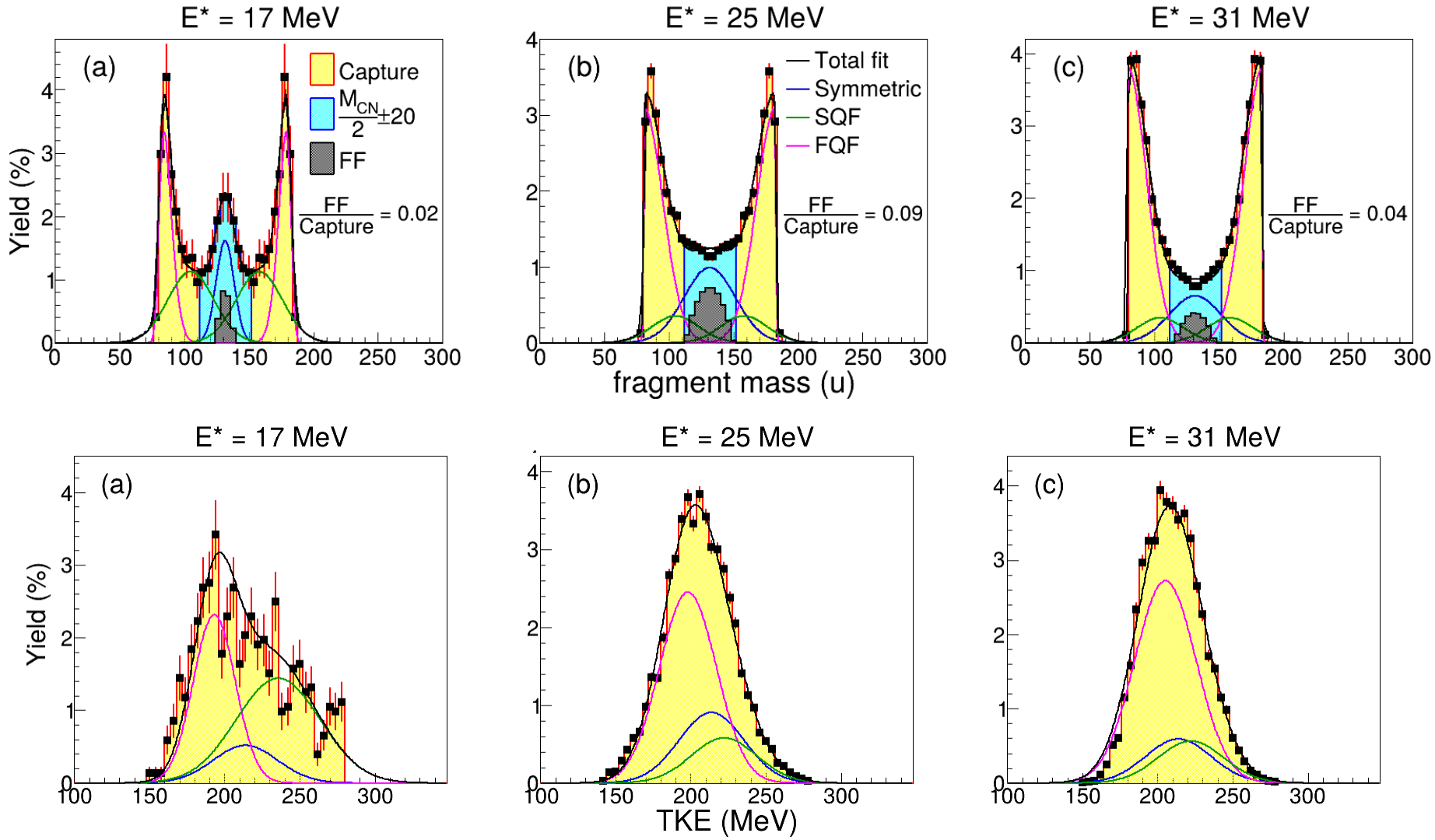
$$A_{subtracted}^{Integral} \geq A_{subtracted}^{Bin-by-bin} \geq A_{subtracted}^{Maximal}$$

$$A_{FF}^{Integral} \leq A_{FF}^{Bin-by-bin} \leq A_{FF}^{Maximal}$$

$$\Rightarrow \quad P_{CN}^{Integral} < P_{CN}^{Bin-by-bin} \leq P_{CN}^{Maximal} < P_{CN}^{YF}$$

$$\boxed{P_{CN}^{Central} = \frac{P_{CN}^{Integral} + P_{CN}^{Bin-by-bin}}{2}}$$

Fit to the mass dist. and area-normalized model overlay on TKE distributions of $^{54}Cr+^{209}Bi \rightarrow {}^{263}Bh$ at E_{beam}= 261, 271, and 278 MeV



A model-independent quantification of the interplay between the dominant SQF and subleading SS modes remains an open challenge.

T. Banerjee, E. Vardaci, A. Di Nitto et al., Phys. Rev. Lett. 137, 062501 (2026)

Methods for extracting FF

E_{lab} (MeV)	$E_{c.m.}$ (MeV)	E^* (MeV)	Modes	σ_m (u)	$\langle M_i \rangle$	$\langle M_i \rangle_{PES}$ TCSM [39]	σ_{TKE} (MeV)	$\langle TKE \rangle$ (MeV)
260.1	206.7	17.0	Symmetric	7.0 ± 0.9	131.5†	131.5	21.7	213.7
			SQF	18.0†	158.0†	160.0	28.0	235.5
			FQF	8.0 ± 0.5	182.5 ± 0.5 (LP)	180.0	14.0	193.0
270.1	214.7	25.0	Symmetric	19.9†	131.5†	131.5	21.8	213.7
			SQF	18.0†	158.0†	160.0	22.0	222.0
			FQF	15.0 ± 0.2	182.8 ± 0.1 (LP)	180.0	19.0	198.0
277.1	220.2	30.5	Symmetric	20.0†	131.5†	131.5	22.0	213.7
			SQF	18.0†	158.0†	160.0	22.0	222.0
			FQF	14.7 ± 0.2	183.9 ± 0.2 (LP)	180.0	20.5	205.0

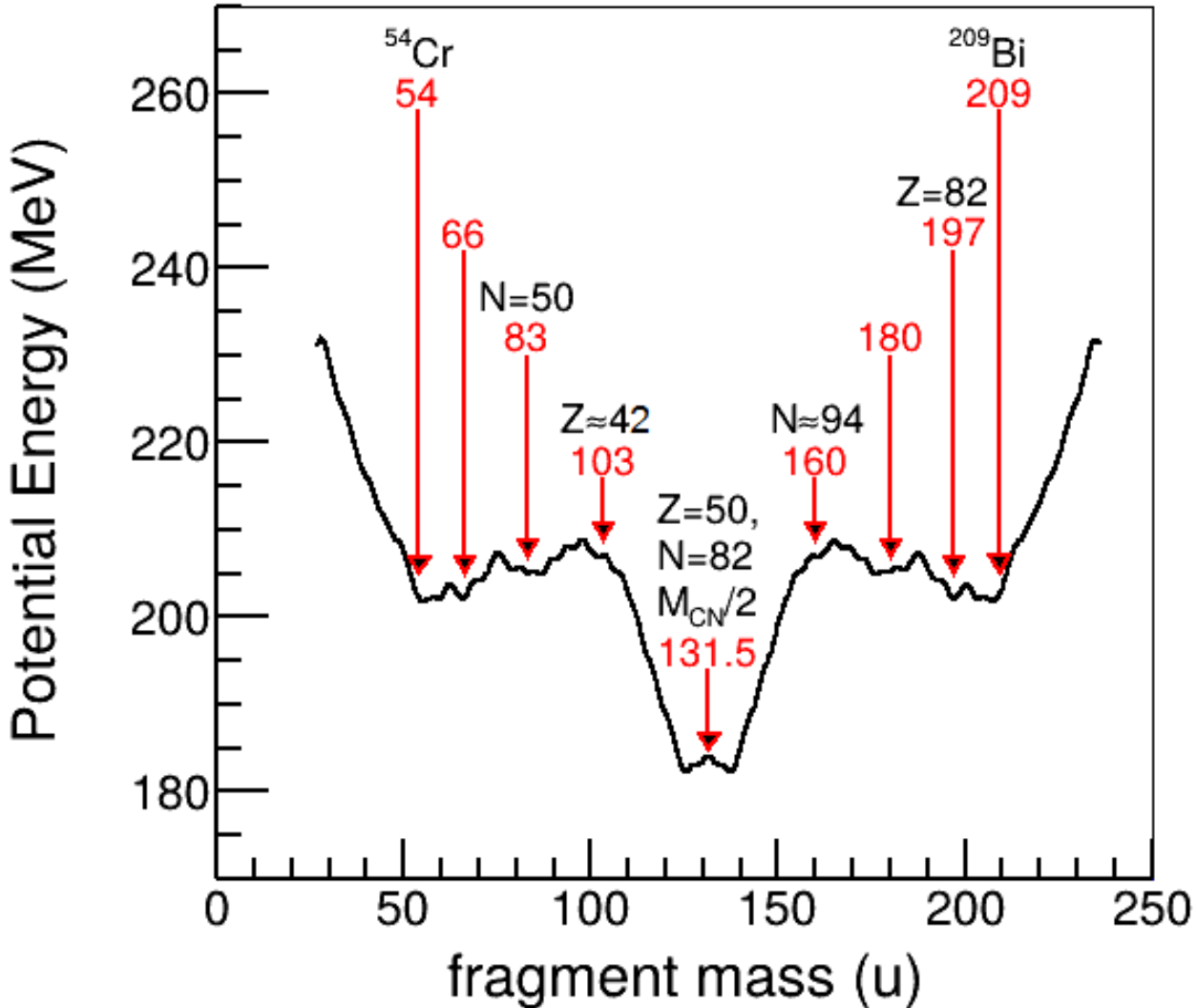
- Consistent with the mean masses corresponding to the secondary minima on the potential energy surface (PES) calculated using the TCSM.

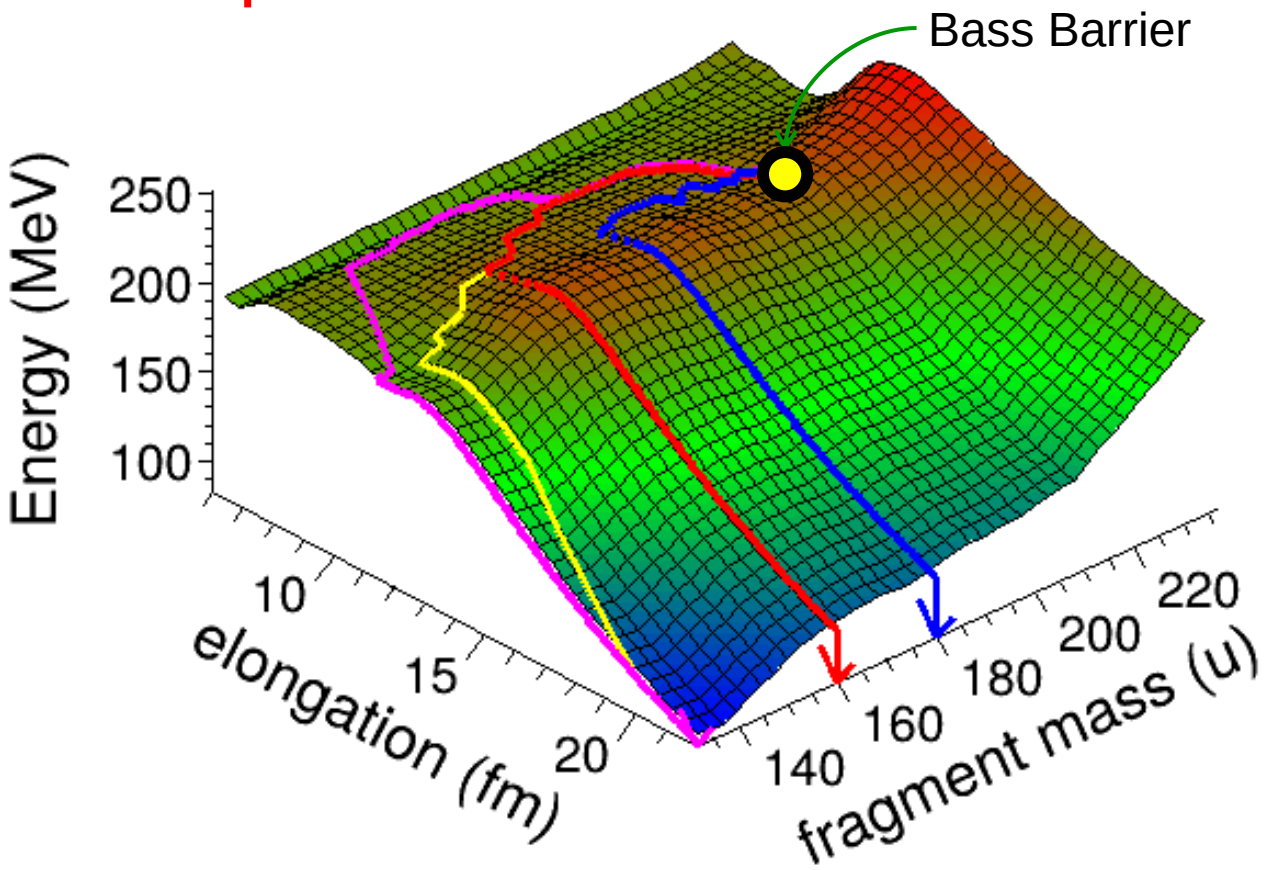
- The theoretical calculations are used strictly as a post hoc physical interpretation.

T. Banerjee, E. Vardaci, A. Di Nitto et al., Phys. Rev. Lett. 137, 062501 (2026)

Potential energy surface of ^{263}Bh and possible active shells

T. Banerjee, E. Vardaci, A. Di Nitto et al., Phys. Rev. Lett. 137, 062501 (2026)
TCSM, Joint Institute for Nuclear Research, Nuclear Reactions Video (NRV), http://nrv.jinr.ru/nrv/webnrv/driving/



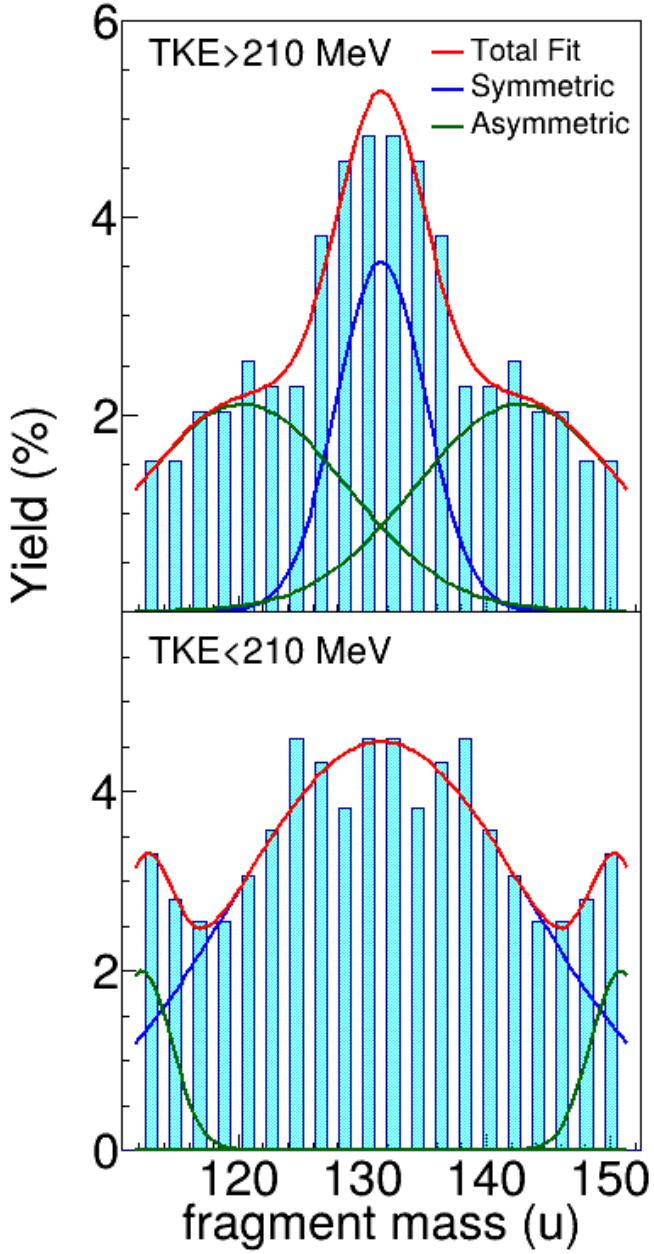


- The trajectories indicate possible fusion-fission (magenta) and quasifission (blue line for asymmetric, and red, and yellow lines for symmetric quasifission) exit channels to guide the eye;

- Actual paths require dynamical modeling

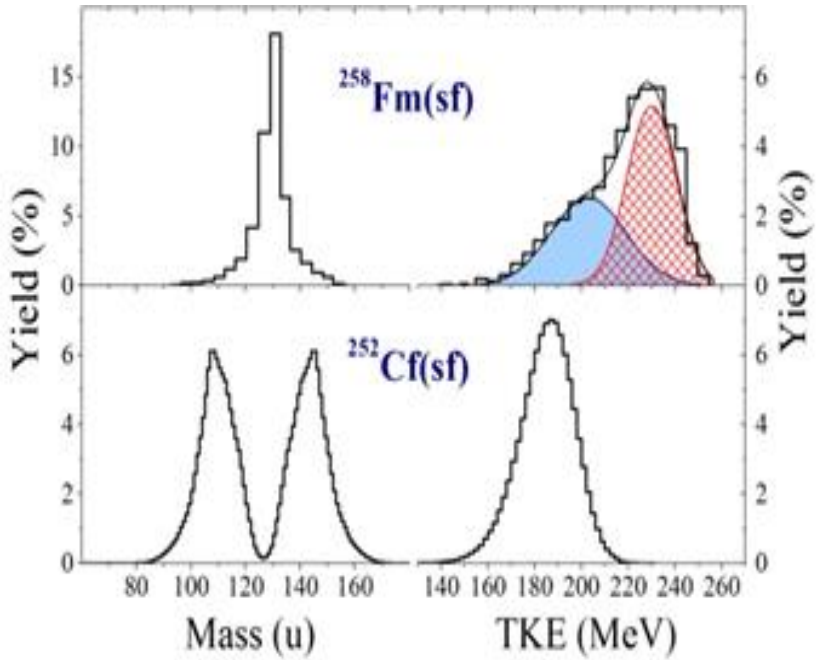
$$(Z_L/M_L) \approx (Z_H/M_H) \approx (Z_{CN}/M_{CN}).$$

High-TKE correlated narrow mass mode in $^{54}Cr+^{209}Bi \rightarrow {}^{263}Bh$



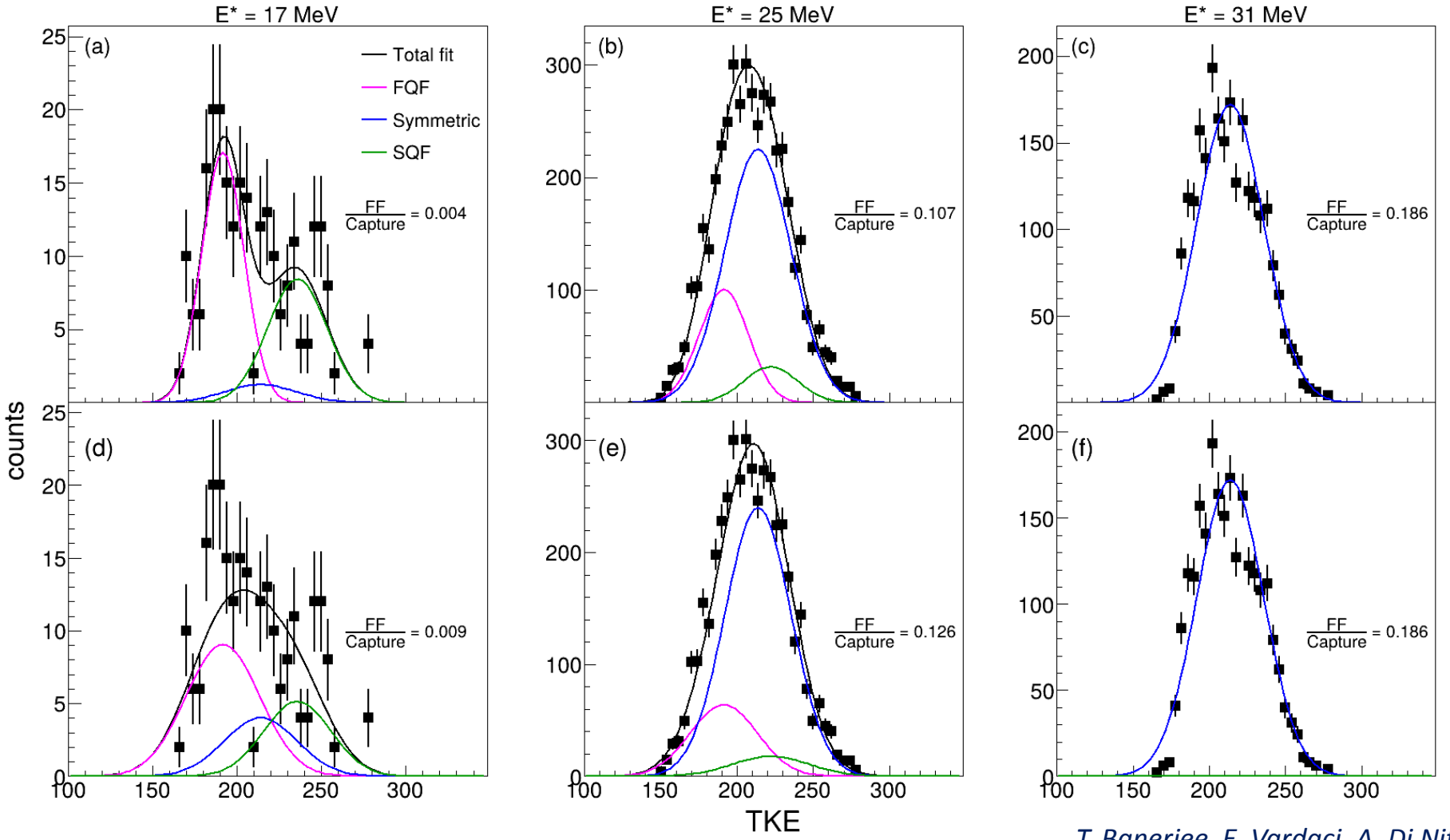
- At the lowest energy, the symmetric mode exhibits a narrow, super-short-like width and high correlated TKE, likely influenced by Z=50, N=82 shells.

- At higher energies the FF residual distributions remain comparably narrow after tail subtraction.



U. Brosa, S. Grossmann, and A. Müller, Phys. Rep. 197, 167 (1990)
E. K. Hulet et al., Phys. Rev. C40, 770 (1989)
T. Banerjee, E. Vardaci, A. Di Nitto et al., Phys. Rev. Lett. 137, 062501 (2026)

Decomposition of symmetric mass gated TKE distributions of $^{54}Cr+^{209}Bi \rightarrow {}^{263}Bh$



Modes	E* 17.0 (MeV)	25.0 (MeV)	30.5 (MeV)
FQF	12.4±1.1	16.1†	-
Symmetric	21.7†	21.8†	22.0†
SQF	17.7±1.7	17.7†	-

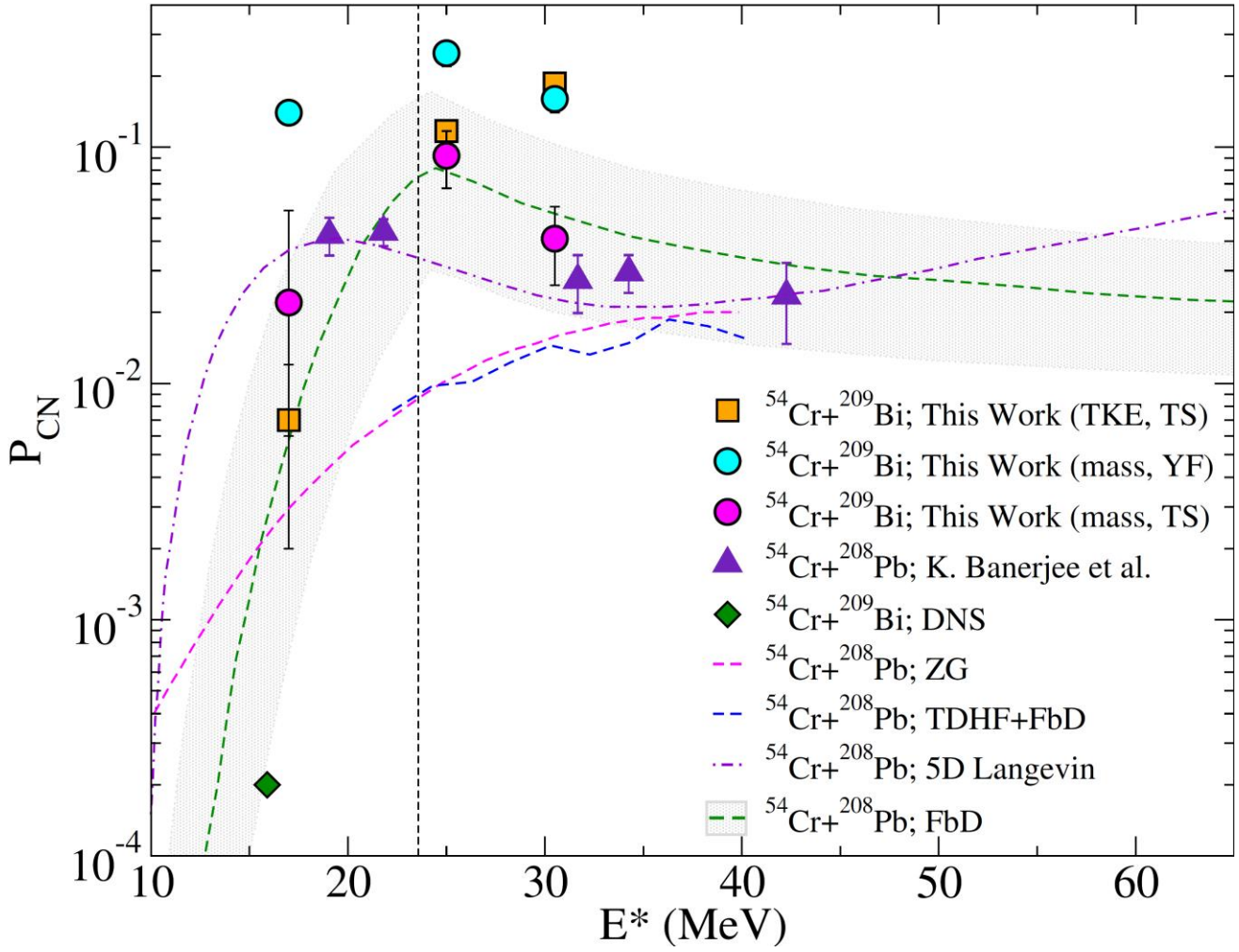
T. Banerjee, E. Vardaci, A. Di Nitto et al., Phys. Rev. Lett. 137, 062501 (2026)

E. M. Kozulin et al., Phys. Lett. B 686, 227 (2010)

M. G. Itkis and A. Y. Rusanov, Phys. Part. Nucl. 29, 160 (1998)

V. E. Viola, Nucl. Data Sheets Sect. A 1, 391 (1965)

Fusion probability of $^{54}Cr+^{209}Bi \rightarrow {}^{263}Bh$



T. Banerjee, E. Vardaci, A. Di Nitto et al., Phys. Rev. Lett. 137, 062501 (2026)

- P_{CN} peaks near the barrier and decreases on either side, with a slower decrease at the above-barrier energy.
- Mostly consistent with that of the FbD model by Cap et al.
- Systematic uncertainty of P_{CN}:
  - Residual variations of the "trapezoidal" gate width
  - Sensitivity to model assumptions

K. Banerjee et al., Phys. Rev. Lett. 122, 232503 (2019)
T. Cap et al., Phys. Rev. C 105, L051601 (2022)
M. Albertsson et al., Phys. Rev. C 110, 014624 (2024)
G. G. Adamian et al., Nucl. Phys. A678, 24 (2000)
X.-X. Sun and L. Guo, Phys. Rev. C 105, 054610 (2022)
V. Zagrebaev and W. Greiner, Phys. Rev. C 78, 034610 (2008)

Summary

- **MTKE distributions measured** for $^{54}Cr+^{209}Bi$ at 261, 271, and 278 MeV using TOSCA.

- **Two asymmetric mass modes observed:** ~80 u (compl. ~183 u), and ~105 u (compl. ~158 u)
  - potentially linked to N=50 and Z≈42/N≈94 shell effects.

- **At the lowest energy:** a narrow, **super-short-like symmetric** mode with **high correlated TKE**
  - likely influenced by Z=50, N=82 shells.

- **At higher energies:** FF residual mass dist. **remain remarkably narrow** after refined tail subtraction.

- **P_{CN} peaks near the barrier** and decreases on both sides, with a **slower decline above the barrier**.

- **Unexpected result:** no clear sub-barrier fusion enhancement, contrary to the earlier PRL result
  - An open question for further investigation.

Participants: T. Banerjee[1]; E. Vardaci[2,1]; A. Di. Nitto[2,1]; P.A. Setaro[2,1]; Giuseppe Alifano[2,1], Davide Panico[2], Simona Di Costanzo[2], Antonio Vanzanella[1], D. Kumar[3], W. H. Trzaska[4], C. Petrone[5], S. Calinescu[5], and C. Borcea[5]

[1]*Istituto Nazionale di Fisica Nucleare, Sezione di Napoli, Napoli, 80126, Italy*
[2]*Dipartimento di Fisica "E. Pancini", Università di Napoli Federico II, Napoli, 80126, Italy*
[3]*GSI Helmholtz Centre for Heavy Ion Research GmbH, Darmstadt, 64278, Germany*
[4]*Department of Physics, University of Jyväskylä, 40014 Jyväskylä, Finland*
[5]*Horia Hulubei National Institute of Physics and Nuclear Engineering, 077125 Bucharest-Mágurele, Romania*



THANK YOU